Prospects and Limitations of Power Balance Approach for Studying Forces and Electromagnetic Damping in Electrical Machines

Bishal Silwal[1,3], Paavo Rasilo[1,2], and Antero Arkkio[1]

[1]Department of Electrical Engineering and Automation, Aalto University, Finland
[2]Laboratory of Electrical Energy Engineering, Tampere University of Technology, Finland
[3]Department of Electrical Energy, Metals, Mechanical Constructions and Systems, Ghent University, Belgium

Cage induction machine with dynamic rotor eccentricity is considered. In general, force and torque computation in the finite element analysis of electrical machines is done using conventional direct methods. Many methods have been put forward with a claim to be more accurate than one another. In this paper we assess the accuracy of the typical force computation method used in the finite element analysis of electrical machines, for various types of mesh used in the machine's air gap during simulations. The possibility of using the power balance of the machine to validate the force calculation and alternatively calculate the force is discussed. Besides, its applicability to study the electromagnetic damping of mechanical vibrations due to unbalanced magnetic pull is presented.

Index Terms—**Cage induction machine, eccentricity, finite element method (FEM), force computation, meshing, power balance.**

I. INTRODUCTION

IN GENERAL, the force computation in an electrical machine can be divided into two categories. First, the computation of force as a global quantity, that is, acting on a body and second, the computation of local forces, for instance, force density on the surface of a material [1]. Many methods have been put forward in the course of time to compute both global and local forces. In this study we focus on the computation of the global force acting on the rotor of the machine based on 2D-FEM. In the finite element analysis of an electrical machine, Maxwell stress tensor method [2] given by (1), or its variant proposed by Arkkio [3] given by (2) and Coulomb's virtual work method [4] given by (3) are commonly used for the calculation of force.

$$F = \int_S \boldsymbol{\sigma}_{\mathrm{M}} \cdot \mathrm{d}\mathbf{S} \qquad (1)$$

$$F = \frac{l}{r_{\mathrm{s}} - r_{\mathrm{i}}} \int_{S_{\mathrm{ag}}} \boldsymbol{\sigma}_{\mathrm{M}} \cdot \mathrm{d}\mathbf{S} \qquad (2)$$

$$F_{\mathrm{x,y}} = \frac{l}{\mu_0} \sum_{e=1}^{N_{\mathrm{eag}}} \int_{\Omega_e} \left[-\boldsymbol{B}^{\mathrm{T}} \boldsymbol{G}^{-1} \frac{\partial \boldsymbol{G}}{\partial x, y} \boldsymbol{B} + \frac{1}{2} B^2 |\boldsymbol{G}|^{-1} \frac{\partial |\boldsymbol{G}|}{\partial x, y} \right] d\Omega \qquad (3)$$

In (1), the Maxwell stress tensor $\boldsymbol{\sigma}_{\mathrm{M}}$ is integrated over the air gap. S is the area of integration. In (2), the area of integration is

confined within a region defined by two concentric boundaries with radii r_{s} and r_{i}, in the air gap. S_{ag} is the cross-sectional area of the integration region. In (3) the force is obtained as the derivative of the energy with respect to the virtual displacement. $\boldsymbol{B}$ is the magnetic flux density, $\mathbf{G}$ is the Jacobian matrix of isoparametric mapping, μ_0 is the permeability of free space, Ω_e is the domain of the element with index e and N_{eag} is the number of elements used in the integration.

The Maxwell stress tensor method is very sensitive to the finite element discretization around the object where the force has to be calculated and the sharp change in the magnetic field in the iron-air interface could result in large error in the calculated force. More reliable results for force are obtained if (2) is used. However, this method is also not very accurate in case of rotor eccentricity as the air gap is non-uniform. Nonetheless, a uniform region with concentric radii can be formed in the air gap to obtain accurate results. For the same kind of finite element discretization used, Coulomb's method yields more accurate result than the Maxwell stress tensor method [5].

In the last decade, a more general approach to calculate the force has been commonly used, called the Eggshell method [7]. This method is based on introducing a thin layer or shell surrounding the object and a smoothing function γ such that the value of γ is 1 on the internal boundary of the shell and 0 on the outer boundary. The force is then calculated by the integral

$$F = \int_V \boldsymbol{\sigma}_{\mathrm{M}} \cdot \nabla \gamma dV \qquad (4)$$

where $\boldsymbol{\sigma}_{\mathrm{M}}$ is the Maxwell stress tensor, V is the volume of the shell. It can be shown that this method is equivalent to the Maxwell stress tensor method and the Coulomb's method. However, it is advantageous in regards to its very general concept [1].

Among other methods, the equivalent magnetizing current method for force calculation was presented in [8]. The main

idea is to replace a magnetic material with a non-magnetic material, having a superficial distribution of the force density. The force is then integrated from the force density. The authors conclude that the method yields similar results to the Maxwell stress tensor for total force, but the results differ in case of local force computation.

The finite element discretization of the problem is a key issue in force computation. Especially, the accuracy of the computation methods is very much affected by the density of the mesh. A dense mesh ensures some degree of accuracy, but the problem can become computationally expensive. Simulations with less computational burden are desired, especially when dealing with optimization problems using FEM. In such case, the choice of a mesh that gives the result with sufficient accuracy in reasonable amount of computation time becomes important. Improved results in terms of mesh-sensitivity has been presented in [5] which uses the same basic principle as the conventional methods like the Maxwell stress tensor method and Coulomb's method, with an addition that the integration is done in multiple layers. The error in the force computation due to discretization is discussed in [6, 9] and an error estimator has been presented.

Recently, the authors studied comprehensively the influence of the air gap mesh on the calculation of the electromagnetic torque [10]. The authors also presented an approach to compute the average torque of the machine from the power balance. The power balance method was compared with the Coulomb's method based on different types of finite element mesh in the air gap and it was seen that it resulted in the average torque that is not affected by the change in the mesh. At the same time, the torque from the Coulomb's method was seen to vary with the type of mesh and also the shape of elements used in the computation. Therefore, a similar effect as in the torque computation could be expected in the force computation from the Coulomb's method.

For a cage induction machine with eccentric rotor, the numerical power balance has already been a topic of discussion in [11]. In an eccentric machine, the tangential force component combines with the whirling motion to produce a power which is also transferred to or from the system, depending on the direction of the force. This power is very small in comparison to the power transmitted by the shaft. However, the knowledge of this small power termed as "whirling power" will lead to an approach to compute the force, which is presented in this paper.

In this paper, the power balance approach and its prospects to calculate force and study electromagnetic damping of the mechanical vibrations will be presented first. Second, the influence of air gap mesh on the computation of force in cage induction machines will be presented for both Coulomb's method and the power balance approach. Then the effect of the electromechanically induced damping on the mechanical vibration will be illustrated.

II. POWER BALANCE APPROACH

The power balance expression of a healthy cage induction motor can be written as

$$P_{in} = P_{loss} + \frac{dW_f}{dt} + T\omega_m \qquad (5)$$

where P_{in} is the electric input power, P_{loss} is the electromagnetic loss, W_f is the magnetic energy and $T\omega_m$ is the output power transmitted through the shaft. This expression was integrated over a time interval in order to obtain the average torque over the interval in [10]. As mentioned in the previous section, when the machine is under dynamic eccentricity, the force combines with the whirling motion to transfer some power, which is termed as the whirling power. Thus, the above power balance is not valid for an eccentric machine. The power transferred by the force should also be taken into account, such that the power balance expression becomes

$$P_{in} = P_{loss} + \frac{dW_f}{dt} + T\omega_m + P_{whirl} \ . \qquad (6)$$

The whirling power can be determined from the power balance or from the force computed from any conventional direct method. For instance, if $\mathbf{F}$ is the force vector obtained from (3) and $\mathbf{v}$ is the whirling velocity vector, the whirling power can be obtained as

$$P_{whirl} = \mathbf{F} \cdot \mathbf{v} \qquad (7)$$

If ε is the eccentricity and δ is the radial air gap length and ω_w is the whirling frequency, the position of the rotor and the velocity vector of whirling is obtained as

$$p_c = \frac{\varepsilon\delta}{2} e^{j\omega_w t}$$
$$\mathbf{v} = \dot{p}_c \qquad (8)$$

There are three prospects of (6). First, it can be used to validate the force (tangential component because the radial force component is perpendicular to the whirling motion therefore do no contribute to the whirling power) computed by other existing force computation method. For this the whirling power computed from (7) is validated against the whirling power computed from (6). Second, the whirling power computed from (6) can alternatively be used to calculate the tangential component of the force. Third, since the whirling power acts as either a stabilizing power or destabilizing power depending if the force is positive or negative, it can be used to study electromagnetic damping of rotor vibrations.

The power terms in (6) are calculated as the change in energy in a certain time interval which is explained in detail in [10]. The power balance approach is implemented in FEM and the method used for the FEM is explained in the next section.

III. FINITE ELEMENT ANALYSIS

A two-dimensional time-stepping finite element analysis is used to obtain the magnetic field solution. The time-stepping method is based on the A–Φ formulation where A is the

magnetic vector potential and Φ is the reduced electric scalar potential. The Maxwell field equations in the quasi-static state together with the constitutive material equations leads to the following equation to be solved in the cross-sectional geometry of the machine.

$$\nabla \times (\upsilon \nabla \times A) = -\sigma \left(\frac{\partial A}{\partial t} - \nabla \Phi \right) \qquad (9)$$

where, υ is the reluctivity and σ is the conductivity of the material. The field in the end-windings is taken into account by adding an impedance to the circuit equations of the windings. The circuit equations are then solved simultaneously with the field equations. The magnetic non-linearity in the materials is modeled by using a single valued magnetization curve. For all time integrations, Trapezoidal rule has been used. The details of the finite element method used in this paper can be found in [3].

The rotor center position is forced to move along a circular path at a constant speed to model the whirling motion of the rotor. The radius of the circular path is equal to the eccentricity expressed as a percentage of the radial air gap length. For instance, if the eccentricity is set to 11%, the whirling radius equals 11% of radial air gap length. In addition, the rotor is rotated in its mechanical angular speed, which is modeled by the moving-band technique.

IV. INFLUENCE OF AIR GAP MESH

The parameters of the machines studied are shown in Table I. The mesh used in this paper consists of second order triangular elements. A typical mesh for the given 37 kW machine has about 14000 to 28000 elements and 18000 to 36000 nodes. The exact number will depend on the density of the mesh in the air gap. In this paper the forces are calculated for different variations of the mesh. Figure 1 shows a quarter of the typical mesh used in the simulations. In the simulations, the mesh in the whole cross-section is used. Different types of mesh are created by changing the number of layers of elements in the air gap of the machine. More mesh variations can be produced by changing the band of elements used for the rotation of the rotor and force computation. Altogether 14 different combinations of mesh are made and used in the simulations by changing the number of bands of elements and the bands that are used for the rotation of the rotor and force computation. The mesh combinations are explained figuratively in Figure 2. For example, in combination index 1, only one layer of element is used and both the rotation and force computation is done from the same layer, while for combination index 4, two layers are used, the second layer is used for rotation and the first layer is used for force computation. The number of elements and nodes in the mesh increases with the increase in the number of bands in the air gap.

In ideal case, the force should not vary if the air gap mesh used in the simulations changes. Figure 3 shows the radial and the tangential components of the force computed for all 14 mesh combinations for the 37 kW induction machine when supplied by the rated supply voltage at rated load. The eccentricity in this case is set to 33% of the air gap. The forces

are calculated by using Coulomb's method (3) and shown in the figures as an average force over a time interval. It can be seen how the variations in the air gap mesh result into varying forces. Although the variations are visible, the difference between the maximum and the minimum values of force is not considerably high. The differences between the maximum and the minimum value of the forces in percentage with respect to the mean force among all combinations in each case are shown in Table II. In this case, both for the radial force and the tangential force, the variation is about 0.8 %.

TABLE I
PARAMETERS OF THE TEST MACHINES

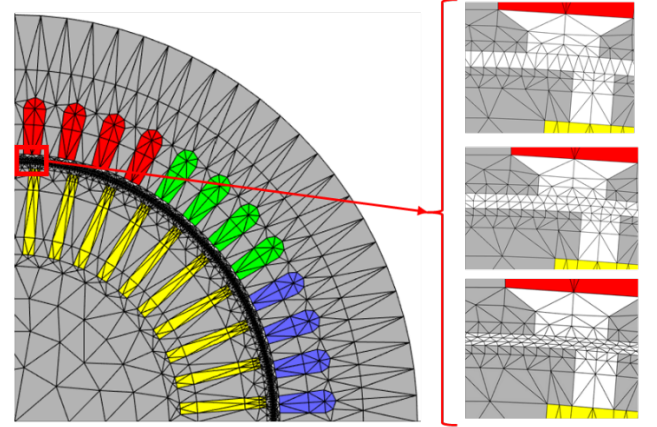| Parameter	Machine I	Machine II
Rated power [kW]	37	15
Connection	Star	Delta
Rated voltage [V]	400	380
Supply frequency [Hz]	50	50
Rated current [A]	70	31
Air gap length (mm)	0.8	0.45
Slip	0.016	0.032
Weight [kg]	63	45

Fig. 1. Typical mesh used in the simulation.

The variations in forces shown in Figure 3 are negligible considering the mean force and also the weight of the rotor. But the situation can get worse if the quality of the mesh is reduced. Next, a 15 kW cage induction machine with a smaller radial air gap length is chosen. For the same type of mesh used, the elements in the 37 kW machine are more uniform, regular and of better quality than in the 15 kW machine which can be seen by comparing the meshes of two machines in Figure 1 and Figure 4. The air gap length of the 15 kW machine is small and also the number of nodes in the stator and rotor surfaces is less compared to the 37 kW machine. This affects the shape and the regularity of the elements. The forces computed for the 15 kW machine are shown in Figure 5. The variations in this case as shown in Table II are 11 % and 7 % for the radial and the tangential force, respectively, which are large than the previous case.
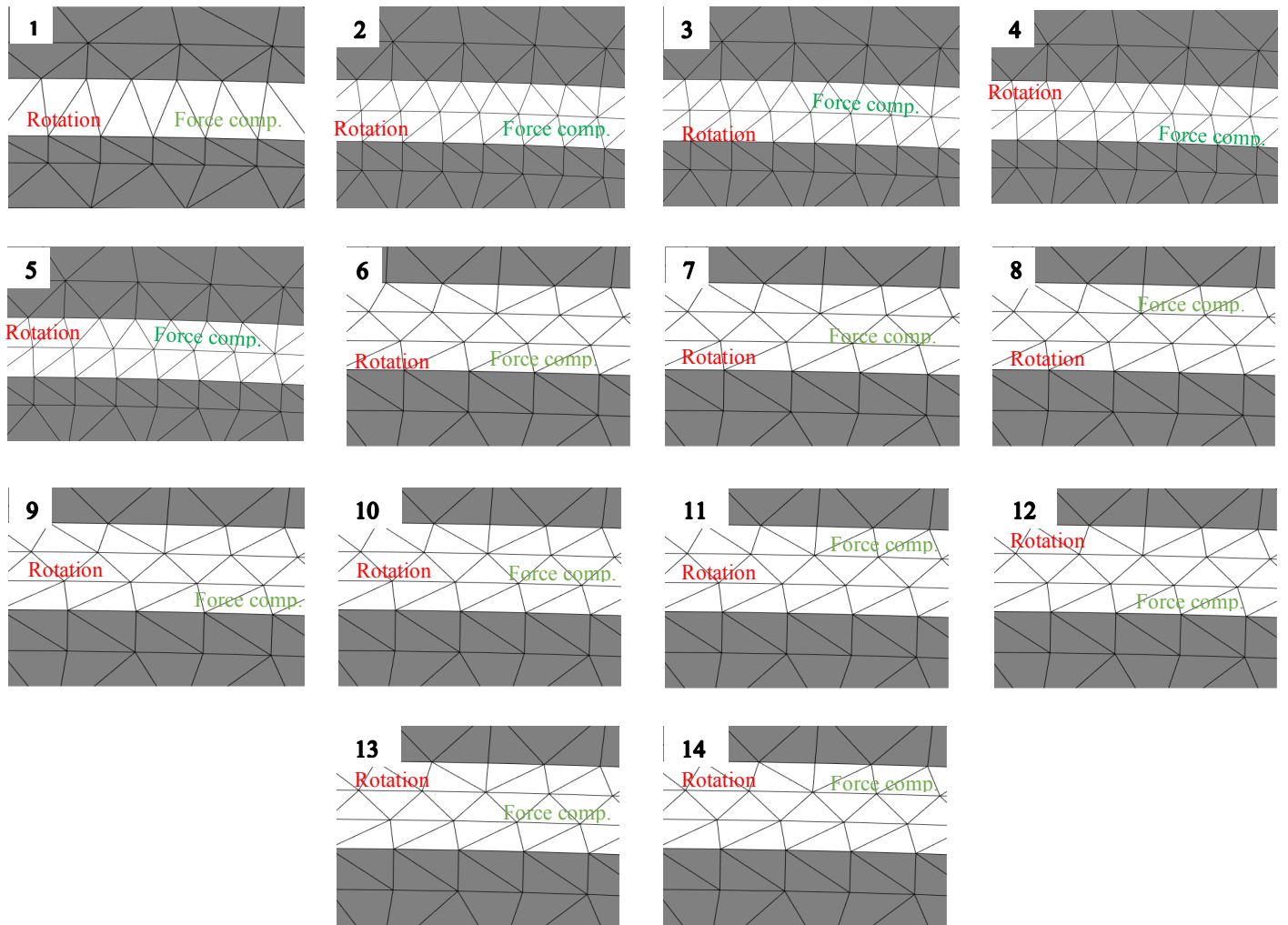
Fig. 2. 14 different variations created by diving the air gap into different layers of elements and by changing the band used for rotation of the rotor and force computation.
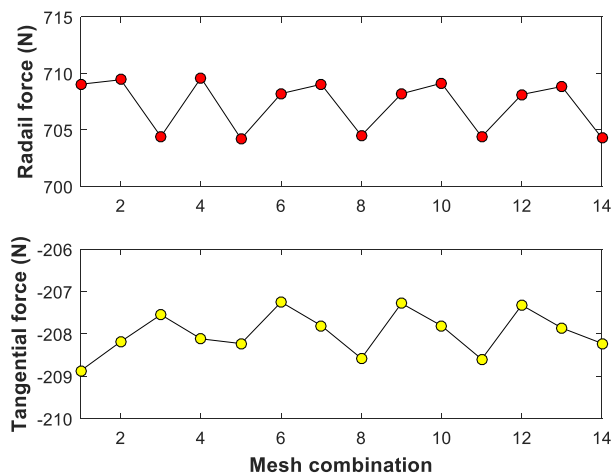

Fig. 3. Eccentricity forces for 37 kW induction machine under 33% dynamic rotor eccentricity computed for different mesh combinations
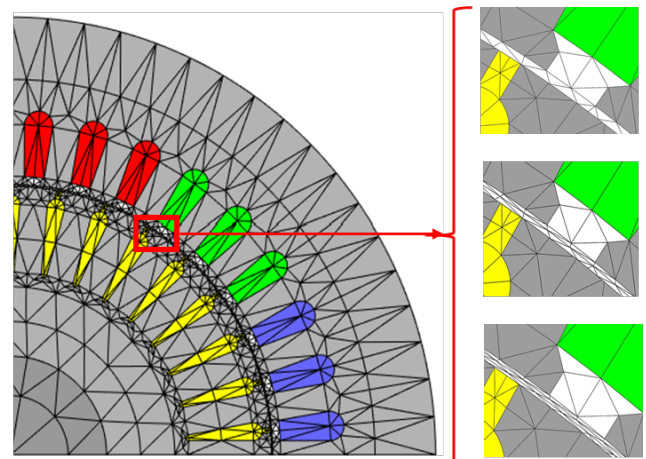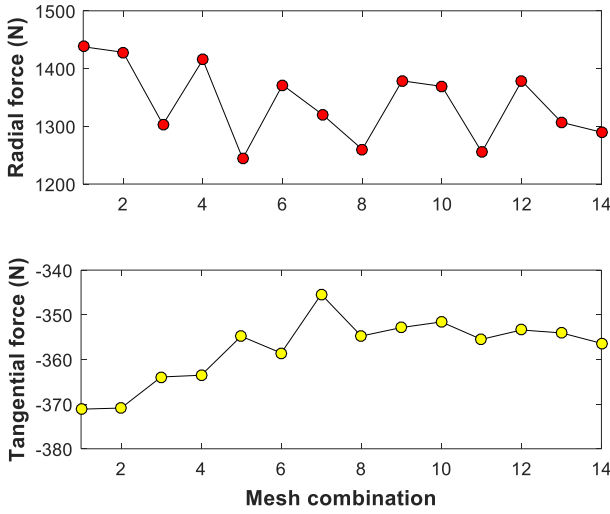

Fig. 4. Mesh used in the simulation of the 15 kW induction machine

TABLE II
DIFFERENCE BETWEEN THE MAXIMUM AND THE MINIMUM VALUE OF THE
FORCE SHOWN IN PERCENTAGE WITH RESPECT TO THE MEAN FORCE AMONG
ALL COMBINATIONS IN EACH CASE

	37 kW Machine Airgap length: 0.8 mm	15 kW Machine Airgap length: 0.45 mm
Mesh combination changed		
Difference in radial force	0.8 %	11 %
Difference in tangential force	0.8 %	7 %
Shape of elements changed		
Difference in radial force	0.08 %	9 %
Difference in tangential force	0.11 %	11 %

the radial force, but the behavior of the force is different. Nevertheless, the difference between the forces is seen to be increasing when changing the shape of the element from equilateral to right-angled triangle.
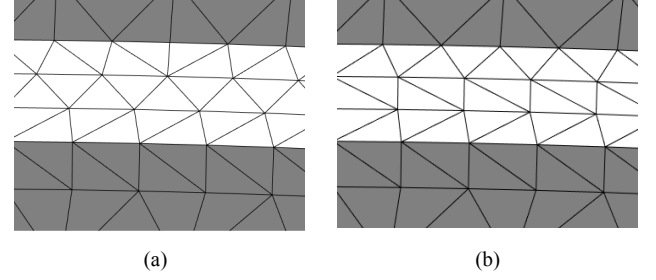

(a)   (b)

Fig. 6 (a) equilateral triangular and (b) right-angled triangular element used in the middle layer for force computation to study the effect of shape of element on computation.
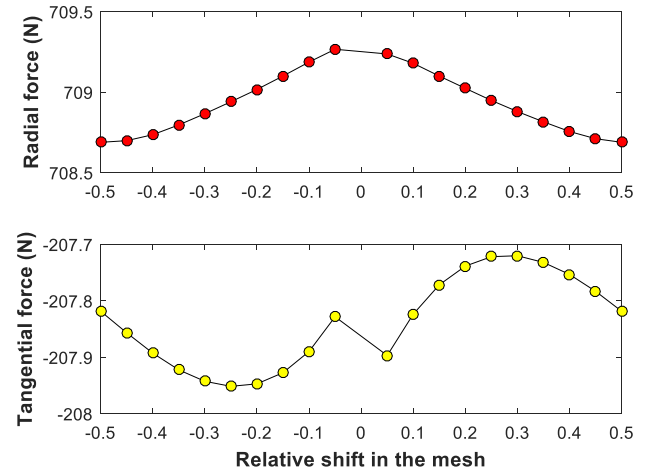

Fig. 5. Eccentricity forces for 15 kW induction machine under 33% dynamic rotor eccentricity computed for different mesh combinations

Fig. 7. Force as a function of the shape of the elements used for force computation. The results shown is for the 37 kW machine

The force is not only affected by the type of mesh used in the simulation but also by the shape of the elements in band in which force is integrated. The influence of the element shape is studied by using a mesh with three layers of elements in the air gap and the middle band used for force computation (mesh combination index 10). First, the machine was simulated with equilateral triangular elements (Figure 6(a)) in the band used for the force computation. Then in each simulation the element sides were shifted such that the equilateral elements were gradually changed to right-angled triangular elements (Figure 6(b)) and then back again to be equilateral.

Figure 7 and Figure 8 show the forces as a function of the shape of the elements. The horizontal axis shows the element sides shift scaled by the length of the element side. ±0.5 shift corresponds to an equilateral triangular element while 0 shift corresponds to a right-angled triangular element. The radial force is seen to have an increasing trend when the element shape is changed from equilateral to right-angled. The variation is again significant in the case of 15 kW machine. The tangential component also shows variations, much smaller compared to
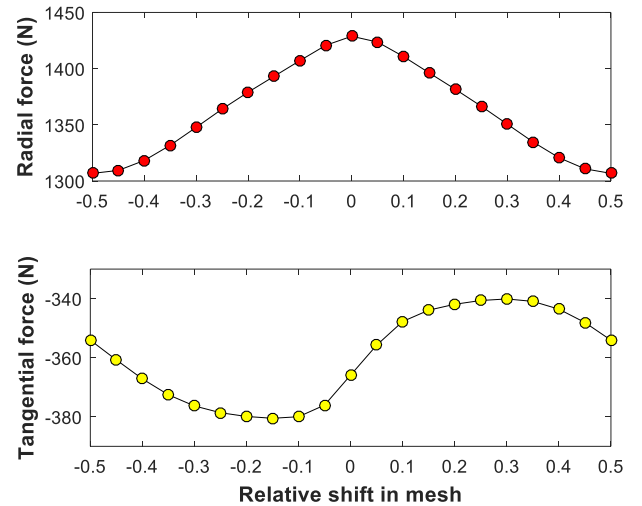

Fig. 8. Force as a function of the shape of the elements used for force computation. The results shown is for the 15 kW machine

As mentioned in the earlier section, the power balance of the machine can be used to validate the force computation methods. For that purpose, the whirling power is calculated by using (7) and then substituted in (6). The power balance error is then calculated. In theory, the error should be zero. Figure 9 shows the power balance errors for different mesh variations, in watts, for 37 kW machine. It can be seen from the result that the power balance is good except for mesh combinations 3, 8, 9, 11 and 12. The reason for large error can be explained by studying the torque. Figure 10 shows the average torque of the machine for different types of finite element mesh. The inaccuracy in the torque describes well the corresponding power balance error shown in Figure 9 in the afore-mentioned mesh combinations.

Based on the results of Figure 9, the power balance can be used to compute the force. The force is deduced from the whirling power. Figure 11 shows the tangential force computed from the power balance. The result is inaccurate in the cases when the torque variations are large. But in other cases, the results show reasonable agreement.
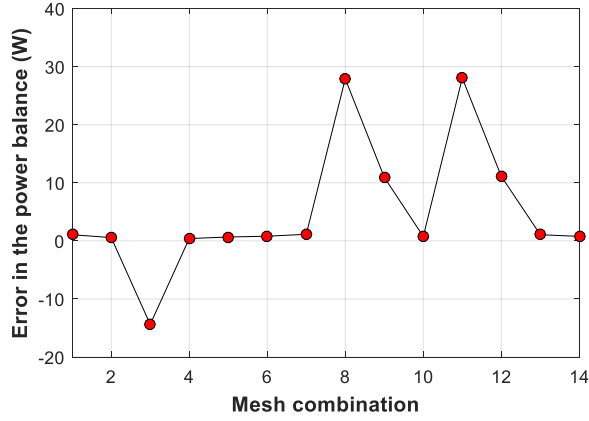

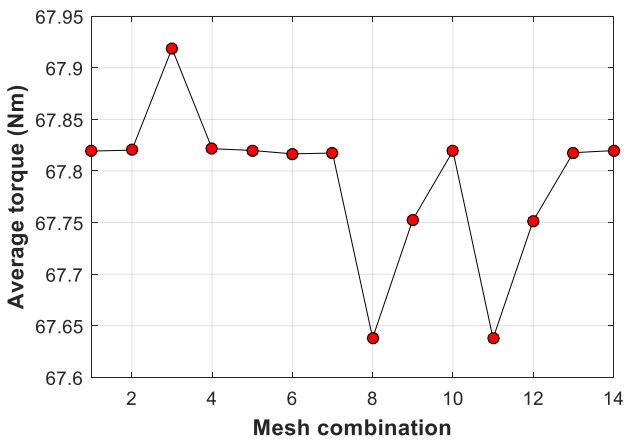Fig. 9. Error in the power balance (6), for 37 kW machine

Fig. 10. Average torque of the 37 kW machine with different mesh combinations

The results shown in Figures 9-11 suggest that using the same band of elements for force computation and for the rotation of the rotor is a good choice. In such mesh combinations, the power balance was seen to be good. The

averaging over all shapes of elements caused by the rotation leads to the reliable value of torque. Therefore, when using the power balance to calculate force, using the same mesh for rotation and for torque computation will ensure good accuracy of torque thus allowing to calculate force from the power balance.
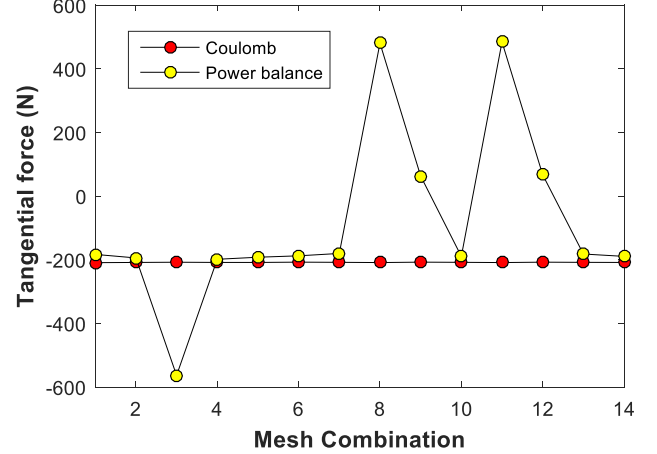

Fig. 11. Force computed from the power balance approach, for 37 kW machine.

V. ELECTROMAGNETICALLY INDUCED DAMPING

To study the electromagnetic damping from the power balance approach, the electromagnetically induced damping (EiD) coefficient in the mechanical model is calculated from the whirling power. The mechanical behavior of the rotor is modeled by using a simple Jeffcott rotor model, shown in Figure 12.
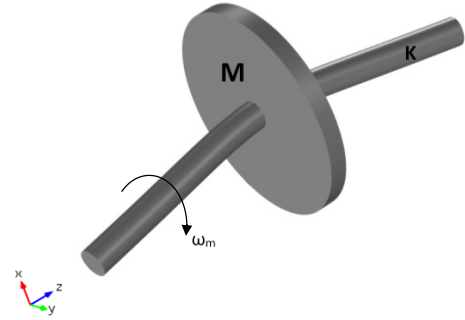

Fig. 12. Jeffcott rotor model

The rotor is modeled as a rigid disc of mass M in the middle of a uniform, massless and flexible shaft with stiffness K. The shaft is supported by rigid bearings at both the ends and the disc is assumed to move only in x-y plane. The Jeffcott rotor model has been commonly used to model the mechanical behavior of the machine when studying the electromechanical interactions in rotordynamics, for cage induction machines, for instance in [12]. If $\bar{p}_c$ defines the center point of the rotor as $\bar{p}_c = x(t) + jy(t), D_m, a, \omega_m$ are the viscous damping from the surrounding fluid, amplitude of the unbalance and the rotor

speed, respectively, the equation for the rotor motion can be given as

$$M\overline{p}_{\mathbf{c}} + \left(D_{\mathrm{m}} - D_{\mathrm{e}}\right)\overline{p}_{\mathbf{c}} + K\overline{p}_{\mathbf{c}} = Ma\omega_{\mathrm{m}}^2 e^{j\omega_{\mathrm{m}}t} \quad (10)$$

The electromagnetically induced damping coefficient can be estimated from the power transferred by the forces as [13]

$$D_{\mathrm{e}} = \frac{2P_{\mathrm{whirl}}}{(a\omega_{\mathrm{m}})^2} \quad . \quad (11)$$

The whirling power computed by using (7) for the 37 kW machine under 33% eccentricity is shown in Figure 13 as a function of the whirling frequency. For this, the rotor was forced to whirl around the stator center-point at the given frequency. The mesh combination 10 is used in the simulations. The figure shows the frequency range near the rated mechanical speed of the rotor, which corresponds to 24.6 Hz. The figure gives an idea about the frequency range when the whirling power acts as a positive damping or a negative damping from the mechanical point of view. When the whirling power is positive, the force is in the same direction of the whirling. Therefore, it adds more power into the whirling causing destabilization. But when the whirling power is negative, it means that the force is in the direction opposite to the whirling motion. This is the case of positive damping from the mechanical point of view.
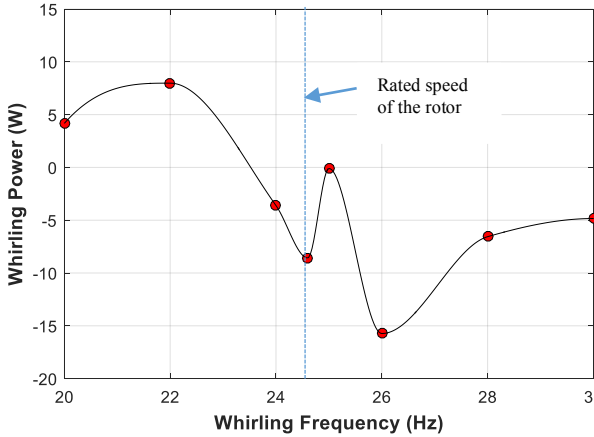

Fig. 13. Whirling power as a function of the whirling frequency, computed by using (7)

Now, the whirling power is computed from the power balance. In this case the whirling frequency is same as the rated mechanical angular frequency of the rotor and eccentricity is set to 33%. The electromagnetically induced damping obtained from the whirling power is substituted in (10) and the mechanical behaviour is observed. The mass of the rotor in this case is 63 kg and the stiffness is 0.15 GN/m. The viscous damping from the surrounding fluid is assumed to be 2000 Ns/m. When the rotor is whirling at the same frequency as the rated speed, the whirling power is negative which means that the damping is positive. The amplitude of the relative displacement is plotted and shown in Figure 14. The curve 'Without EiD' corresponds to the case when the EiD is not

taken into account. The damping of the amplitude at the natural frequency can be seen when the EiD is taken into account curve 'With EiD' in the figure. The case would have been opposite if, for instance, the rotor was whirling at 20 Hz or 22 Hz. In that case, the damping would be negative and the amplitude curve would have amplified instead of being damped, which means that even a small unbalance would cause larger vibrations.
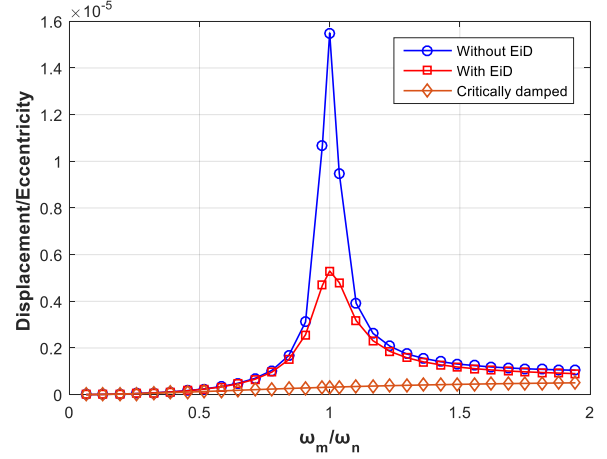

Fig. 14. The response of the mechanical model when the unbalance is equal to 33% of the air gap length of the machine

VI. LIMITATIONS OF THE APPROACH

The potential application of the power balance method to calculate electromagnetic forces in electrical machines and to study the effect of the electromagnetic damping in the mechanical vibrations have been shown in the previous sections. Both prospects are based on the calculation of the whirling power from the power balance. Thus, for the power balance to be used to compute force and to study the damping, an accurate calculation of the whirling power is needed. However, from (6), one can see that both the whirling power and the electromagnetic torque have to be computed at the same time. We have seen that the air gap mesh has considerable influence on the accuracy of the torque computation. In addition, the shape of the elements also affects. Even if the variation in the torque is small, it makes a substantial effect if we consider the magnitude of the whirling power. For example, for a machine rotating at an angular speed of 152 rad/sec, if the torque changes by 0.1 N, the corresponding change in the power becomes 15.2 W, which is significant in this case. Small inaccuracy in the torque will lead to significant difference in the magnitude of the whirling power, which ultimately leads to the inaccuracy in the computed force, which is evident from Figure 11. Therefore, the power balance approach is not yet robust because of the errors associated with the torque. The time integration method also has an effect on the accuracy of the power balance. In this study the Trapezoidal rule has been used for all time integrations. It is known that this method is energy conserving. Some higher order methods for time integration could be tested to confirm more accuracy. If the errors associated with the meshing is minimized, the power balance approach can be useful in the finite element analysis of electrical machines.

REFERENCES

[1] M. vander Giet, D. Franck, F. Henrotte, K. Hameyer, "Comparative study of force computation methods for acoustic analyses of electrical machines," *In Proc. The 14th IGTE Symposium on Numerical Field Calculation in Electrical Engineering: Graz*, Sept. 2010.

[2] A. N. Wignall, A. J. Gilbert, S. J. Yang, "Calculation of forces on magnetised ferrous cores using the Maxwell stress method," *IEEE Trans. Magn.*, vol. 24, no. 1, Jan. 1988.

[3] A. Arkkio, 'Analysis of induction motors based on the numerical solution of the magnetic field and circuit equations', *Acta Polytechnica Scandinavica*, 1987.

[4] J. L. Coulomb, "A methodology for the determination of global electromechanical quantities from a finite element analysis and its application to the evaluation of magnetic forces, torques and stiffness," *IEEE Trans. Magn.*, Vol. 19, No. 6, pp. 2514-2519, Nov. 1983.

[5] S. L. Ho, S. Niu, W. N. Fu and J. Zhu, "A mesh-insensitive methodology for magnetic force computation in finite-element analysis," *IEEE Trans. Magn.*, Vol. 48, No. 2, pp. 287-290, Feb. 2012.

[6] W. N. Fu and S. L. Ho, "Error estimation for the computation of force using the virtual work method on finite element models," *IEEE Trans. Magn.*, vol. 45. no. 3, pp. 1388-1391, Mar. 2009.

[7] F. Henrotte, M. Felden, M. vander Giet and K. Hameyer, "The eggshell approach for the computation of electromagnetic forces in 2D and 3D", *COMPEL: The International Journal for Computation and Mathematics in Electrical and Electronic Engineering*, vol. 23, no. 4, pp. 996-1005, 2004.

[8] G. Hennerger, P. K. Sattler, D. Shen, "Nature of equivalent magnetizing current for the forces calculation", *IEEE Trans. Magn.*, vol. 28, no. 2, pp. 1068-1071,1992.

[9] J. P. Webb, "An estimator for force errors in finite-element analysis", *IEEE Trans. Magn.*, vol. 39, no. 3, pp. 1428-1431, May 2003.

[10] B. Silwal, P. Rasilo, L. Perkkiö, M. Oksman, A. Hannukainen, T. Eirola, A. Arkkio, "Computation of torque of an electrical machine with different types of finite element mesh in the air gap" *IEEE Trans. Magn.*, vol. 50, no. 12, pp. 1-9, December 2014.

[11] B. Silwal, P. Rasilo, L. Perkkiö, A. Hannukainen, T. Eirola and A. Arkkio, "Numerical analysis of the power Balance of an electrical machine with rotor eccentricity," in *IEEE Trans. Magn.*, vol. 52, no. 3, pp. 1-4, March 2016.

[12] T. Holopainen, "Electromechanical interaction in rotordynamics of cage induction motors", *PhD Thesis*, Helsinki University of Technology, Finland, 2004.

[13] T. Holopainen, "Modelling and simulation of multitechnological machine systems", *VTT Symposium 209*, Espoo, Finland, 2001. (Available at: http://www.vtt.fi/inf/pdf/symposiums/2001/S209.pdf)